J|A|C|S
ARTICLES
Published on Web 08/18/2007

High-Enthalpy Hydrogen Adsorption in Cation-Exchanged Variants of the Microporous Metal−Organic Framework $Mn_3[(Mn_4Cl)_3(BTT)_8(CH_3OH)_{10}]_2$

Mircea Dincă and Jeffrey R. Long*

Contribution from the Department of Chemistry, University of California, Berkeley, California 94720

Received April 24, 2007; E-mail: jrlong@berkeley.edu

Abstract: Exchange of the guest Mn^{2+} ions in $Mn_3[(Mn_4Cl)_3(BTT)_8(CH_3OH)_{10}]_2$ (**1-Mn**$^{2+}$; BTT = 1,3,5-benzenetristetrazolate) with selected cations results in the formation of isostructural framework compounds **1-M** (M = Li^+, Cu^+, Fe^{2+}, Co^{2+}, Ni^{2+}, Cu^{2+}, Zn^{2+}). Similar to the parent compound, the new microporous materials are stable to desolvation and exhibit a high H_2 storage capacity, ranging from 2.00 to 2.29 wt % at 77 K and 900 torr. Measurements of the isosteric heat of adsorption at zero coverage reveal a difference of 2 kJ/mol between the weakest and strongest H_2-binding materials, which is attributed to variations in the strength of interaction between H_2 molecules and unsaturated metal centers within each framework. The Co^{2+}-exchanged compound, **1-Co**$^{2+}$, exhibits an initial enthalpy of adsorption of 10.5 kJ/mol, the highest yet observed for a microporous metal−organic framework.

Introduction

Since its origins in the early 1990s,[1] the field of metal−organic frameworks has developed into one of the most active areas of research in materials chemistry. These compounds consist of metal ions or clusters connected through organic bridging ligands into extended one-, two-, or three-dimensional networks. Initially, the materials had little or no applicability, yet they fascinated researchers with their aesthetically pleasing crystal structures reminiscent of the high-symmetry structures of zeolites.[2] The past decade has seen, however, the emergence of a new generation of metal−organic frameworks, certain of which have shown promise for applications such as gas storage and separation,[3] catalysis,[4] chemical sensing and luminescence,[5] and magnetism.[6] Among these, reports of reversible uptake of hydrogen at cryogenic temperature have sparked keen interest in developing microporous metal−organic frameworks as hydrogen storage materials for mobile applications.[7]

(1) (a) Hoskins, B. F.; Robson, R. *J. Am. Chem. Soc.* **1989**, *111*, 5962−5964. (b) Hoskins, B. F.; Robson, R. *J. Am. Chem. Soc.* **1990**, *112*, 1546−1554. (c) Abrahams, B. F.; Hoskins, B. F.; Liu, J. L.; Robson, R. *J. Am. Chem. Soc.* **1991**, *113*, 3045−3051. (d) Abrahams, B. F.; Hoskins, B. F.; Robson, R. *J. Am. Chem. Soc.* **1991**, *113*, 3606−3607. (e) Fujita, M.; Kwon, Y. J.; Washizu, S.; Ogura, K. *J. Am. Chem. Soc.* **1994**, *116*, 1151−1152.

(2) See: (a) Database of Zeolite Structures. http://www.iza-structure.org/databases/ (accessed April 2007). (b) Web page for the Reticular Chemistry Structure Resource. http://rcsr.anu.edu.au/ (accessed April 2007).

(3) (a) Li, H.; Eddaoudi, M.; O'Keeffe, M.; Yaghi, O. M. *Nature* **1999**, *402*, 276−279. (b) Dybtsev, D. N.; Chun, H.; Yoon, S. H.; Kim, D.; Kim, K. *J. Am. Chem. Soc.* **2004**, *126*, 32−33. (c) Dincă, M.; Long, J. R. *J. Am. Chem. Soc.* **2005**, *127*, 9376−9377. (d) Millward, A. R.; Yaghi, O. M. *J. Am. Chem. Soc.* **2005**, *127*, 17998−17999. (e) Mori, W.; Sato, T.; Ohmura, T.; Nozaki, Kato, C.; Takei, T. *J. Solid State Chem.* **2005**, *178*, 2555−2573. (f) Matsuda, R.; Kitaura, R.; Kitagawa, S.; Kubota, Y.; Belosludov, R. V.; Kobayashi, T. C.; Sakamoto, H.; Chiba, T.; Takata, M.; Kawazoe, Y.; Mita, Y. *Nature* **2005**, *436*, 238−241. (g) Chandler, B. D.; Cramb, D. T.; Shimizu, G. K. H. *J. Am. Chem. Soc.* **2006**, *128*, 10403−10412. (h) Pan, L.; Olson, D. H.; Ciemnolonski, L. R.; Heddy, R.; Li, J. *Angew. Chem., Int. Ed.* **2006**, *45*, 616−619. (i) Mueller, U.; Schubert, M.; Teich, F.; Puetter, H.; Schierle-Arndt, K.; Pastré, J. *J. Mater. Chem.* **2006**, *16*, 626−636.

(4) (a) Seo, J. S.; Whang, D.; Lee, H.; Jun, S. I.; Oh, J.; Jeon, Y. J.; Kim, K. *Nature* **2000**, *404*, 982−986. (b) Guillou, N.; Forster, P. M.; Gao, Q.; Chang, J. S.; Nogues, M.; Park, S.-E.; Cheetham, A. K.; Férey, G. *Angew. Chem., Int. Ed.* **2001**, *40*, 2831−2834. (c) Cho, S.-H.; Ma, B.; Nguyen, S. T.; Hupp, J. T.; Albrecht-Schmitt, T. E. *Chem. Commun.* **2006**, 2563−2565. (d) Zou, R.-Q.; Sakurai, H.; Xu, Q. *Angew. Chem., Int. Ed.* **2006**, *45*, 2542−2546. (e) Hasegawa, S.; Horike, S.; Matsuda, R.; Furukawa, S.; Mochizuki, K.; Kinoshita, Y.; Kitagawa, S. *J. Am. Chem. Soc.* **2007**, *129*, 2607−2614. (f) Wu, C.-D.; Lin, W. *Angew. Chem., Int. Ed.* **2007**, *46*, 1075−1078.

(5) (a) Beauvais, L. G.; Shores, M. P.; Long, J. R. *J. Am. Chem. Soc.* **2000**, *122*, 2763−2772. (b) Jianghua, H.; Jihong, Y.; Yuetao, Z.; Qinhe, P.; Xu, R. *Inorg. Chem.* **2005**, *44*, 9279−9282.

(6) (a) Rujiwatra, A.; Kepert, C. J.; Claridge, J. B.; Rosseinsky, M. J.; Kumagai, H.; Kurmoo, M. *J. Am. Chem. Soc.* **2001**, *123*, 10584−10594. (b) Beauvais, L. G.; Long, J. R. *J. Am. Chem. Soc.* **2002**, *124*, 12096−12097. (c) Halder, G. J.; Kepert, C. J.; Moubaraki, B.; Murray, K. S.; Cashion, J. D. *Science* **2002**, *298*, 1762−1765. (d) Maspoch, D.; Ruiz-Molina, D.; Wurst, K.; Domingo, N.; Cavallini, M.; Biscarini, F.; Tejada, J.; Rovira, C.; Veciana, J. *Nat. Mater.* **2003**, *2*, 190−195. (e) Xiang, S.; Wu, X.; Zhang, J.; Fu, R.; Hu, S.; Zhang, X. *J. Am. Chem. Soc.* **2005**, *127*, 16352−16353. (f) Zheng, Y.-Z.; Tong, M.-L.; Zhang, W.-X.; Chen, X.-M. *Chem. Commun.* **2006**, 165−167.

(7) (a) Rosi, N. L.; Eckert, J.; Eddaoudi, M.; Vodak, D. T.; Kim, J.; O'Keeffe, M.; Yaghi, O. M. *Science* **2003**, *300*, 1127−1129. (b) Férey, G.; Latroche, M.; Serre, C.; Millange, F.; Loiseau, T.; Perceheron-Guégan, A. *Chem. Commun.* **2003**, 2976−2977. (c) Pan, L.; Sander, M. B.; Huang, X.; Li, J.; Smith, M.; Bittner, E.; Bockrath, B.; Johnson, J. K. *J. Am. Chem. Soc.* **2004**, *126*, 1308−1309. (d) Rowsell, J. L.; Millward, A. R.; Park, K. S.; Yaghi, O. M. *J. Am. Chem. Soc.* **2004**, *126*, 5666−5667. (e) Lee, E. Y.; Suh, M. P. *Angew. Chem., Int. Ed.* **2004**, *43*, 2798−2801. (f) Dybstev, D. N.; Chun, H.; Kim, K. *Angew. Chem., Int. Ed.* **2004**, *43*, 5033−5036. (g) Zhao, X.; Xiao, B.; Fletcher, A. J.; Thomas, K. M.; Bradshaw, D.; Rosseinsky, M. J. *Science* **2004**, *306*, 1012−1015. (h) Kubota, Y.; Takata, M.; Matsuda, R.; Kitaura, R.; Kitagawa, S.; Kato, K.; Sakata, M.; Kobayashi, T. C. *Angew. Chem., Int. Ed.* **2005**, *44*, 920−923. (i) Chen, B.; Ockwig, N. W.; Millward, A. R.; Contreras, D. S.; Yaghi, O. M. *Angew. Chem., Int. Ed.* **2005**, *44*, 4745−4749. (j) Férey, G.; Mellot-Draznieks, C.; Serre, C.; Millange, F.; Dutour, J.; Surblé, S.; Margiolaki, I. *Science* **2005**, *309*, 2040−2042. (k) Rowsell, J. L. C.; Yaghi, O. M. *J. Am. Chem. Soc.* **2006**, *128*, 1304−1315. (l) Wong-Foy, A. G.; Matzger, A. J.; Yaghi, O. M. *J. Am. Chem. Soc.* **2006**, *128*, 3494−3495. (m) Dincă, M.; Yu, A. F.; Long, J. R. *J. Am. Chem. Soc.* **2006**, *128*, 8904−8913. (n) Ma, S.; Zhou, H.-C. *J. Am. Chem. Soc.* **2006**, *128*, 11734−11735. (o) Latroche, M.; Surblé, S.; Serre, C.; Mellot-Draznieks, C.; Llewellyn, P. L.; Lee, J.-H.; Chang, J.-S.; Jhung, S. H.; Férey, G. *Angew. Chem., Int. Ed.* **2006**, *45*, 8227−8331. (p) Ma, S.; Sun, D.; Ambrogio, M.; Fillinger, J. A.; Parkin, S.; Zhou, H.-C. *J. Am. Chem. Soc.* **2007**, *129*, 1858−1859. (q) Dincă, M.; Han, W. S.; Liu, Y.; Dailly, A.; Brown, C. M.; Long, J. R. *Angew. Chem., Int. Ed.* **2007**, *46*, 1419−1422.

10.1021/ja072871f CCC: $37.00

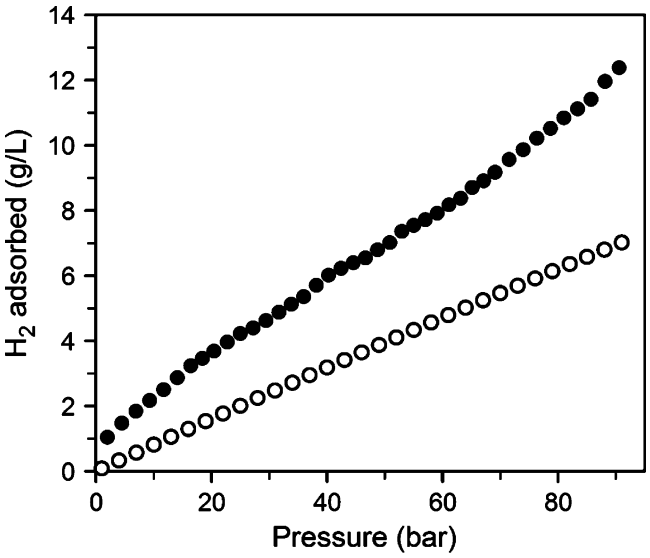

Figure 1. Plot of the total volumetric density of H_2 adsorbed inside **1-Mn^{2+}** at 298 K (●) versus the density of gaseous H_2 under the same temperature and pressure conditions (○).

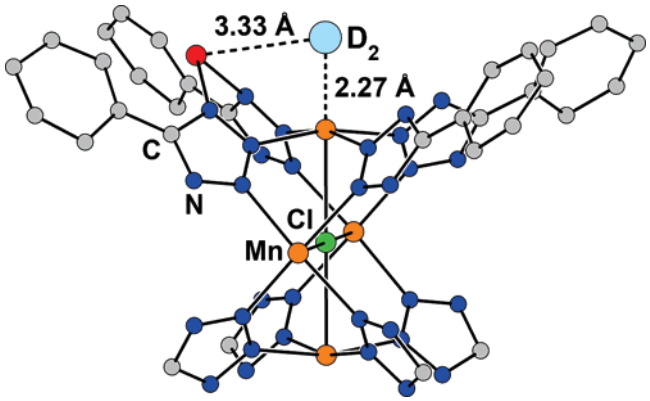

Figure 2. Portion of the crystal structure of **1-Mn^{2+}**, showing the hydrogen adsorption site in the vicinity of coordinatively unsaturated intra- (orange) and extraframework (red) Mn^{2+} ions, as determined using powder neutron diffraction.[8]

Recently, we described the structure and hydrogen sorption properties of the tetrazolate-based metal−organic framework $Mn_3[(Mn_4Cl)_3(BTT)_8(CH_3OH)_{10}]_2$ (**1-Mn^{2+}**, H_3BTT = 1,3,5-tris(tetrazol-5-yl)benzene).[8] This material exhibits a high H_2 adsorption enthalpy of 10.1 kJ/mol and a total H_2 capacity of 6.9 wt % or 60 g/L at 77 K and 90 bar. Adsorption experiments performed at room temperature further revealed a total H_2 uptake of 1.5 wt % at 90 bar (Figure 1), which at 12.1 g/L represents a 77% increase over the density of compressed hydrogen under the same conditions. Powder neutron diffraction experiments showed that the large adsorption enthalpy was due in part to a strong interaction between D_2 molecules and unsaturated Mn^{2+} cations within the anionic framework skeleton. As shown in Figure 2, this strong interaction is also responsible for a short distance of only 2.27 Å between the intraframework Mn^{2+} ions and the D_2 centroids. Notably, charge-balancing, "extraframework" Mn^{2+} cations bound to the N1 and N4 atoms of tetrazolate rings are situated only 3.33 Å from the same D_2 sites, suggesting that they might also contribute to the increased electrostatic potential responsible for the strong binding.

(8) Dincă, M.; Dailly, A.; Liu, Y.; Brown, C. M.; Neumann, D. A.; Long, J. R. *J. Am. Chem. Soc.* **2006**, *128*, 16876−16883.

In view of the recent interest in metal−H_2 binding as a means of increasing the H_2 adsorption energy in metal−organic frameworks,[7i,k,m,p,8,9] we have undertaken a series of cation-exchange experiments, in which solvated **1-Mn^{2+}** is soaked in solutions of Fe^{2+}, Co^{2+}, Ni^{2+}, Cu^{2+}, Zn^{2+}, Li^+, and Cu^+ salts to give the respective ion-exchanged frameworks. Subsequent hydrogen sorption experiments reveal a large cation-dependent variation of the H_2 adsorption enthalpy, indicating a correlation between the nature of the exchanged cation and the strength of H_2 binding. To our knowledge, this represents the first study attempting to vary just the guest cations situated within an anionic metal−organic framework host.

Experimental Section

All reagents were obtained from commercial vendors and, unless otherwise noted, were used without further purification. Compound **1-Mn^{2+}** was synthesized as previously described.[8] Methanol was distilled over Mg/I_2, and CH_3CN was dried over an alumina-packed column before use. Both solvents were degassed by three freeze−pump−thaw cycles, and all manipulations were done under an inert N_2 atmosphere.

General Procedure for the Preparation of the Exchanged Frameworks 1-M (M = Fe^{2+}, Co^{2+}, Ni^{2+}, Cu^{2+}, Zn^{2+}, Li$^+$, Cu$^+$). Crystals of as-synthesized **1-Mn^{2+}** were immersed in concentrated solutions of anhydrous MCl_2 (M = Fe^{2+}, Co^{2+}, Ni^{2+}, Cu^{2+}, Zn^{2+}) or LiCl in freshly distilled methanol. The crystals were soaked for one week, and the solvent was refreshed three times, such that the total soaking time was approximately 1 month. Upon decanting the metal chloride solutions, the cation-exchanged crystals of **1-M** were rinsed and soaked in distilled methanol for 3 days to remove residual free cations from within the pores of **1-M**. A similar procedure using $[Cu(CH_3CN)_4]PF_6$ in CH_3CN was used for the preparation of **1-Cu$^+$**. Elemental microanalyses: For $C_{164}H_{128}Cl_8Fe_4Mn_{24}N_{192}O_{20}$ (**1-Fe^{2+}**·20CH_3OH) calcd: C, 28.41; H, 1.86; N, 38.79; Fe/Mn, 0.169. Found: C, 28.01; H, 1.36; N, 38.81; Fe/Mn, 0.17. For $C_{164}H_{128}Cl_{9.4}Co_{4.7}Mn_{24}N_{192}O_{20}$ (**1-Co^{2+}**·20CH_3OH) calcd: C, 27.99; H, 1.83; N, 38.22; Co/Mn, 0.21. Found: C, 28.39; H, 1.12; N, 38.00; Co/Mn, 0.21. For $C_{164}H_{128}Cl_6Mn_{24.25}N_{192}Ni_{2.75}O_{20}$ (**1-Ni^{2+}**·20CH_3OH) calcd: C, 28.91; H, 1.89; N, 39.46; Ni/Mn, 0.121. Found: C, 28.07; H, 1.55; N, 38.66; Ni/Mn, 0.121. For $C_{164}H_{128}Cl_{10}Cu_{22.4}Mn_{6.6}N_{192}O_{20}$ (**1-Cu^{2+}**·20CH_3OH) calcd: C, 27.17; H, 1.78; N, 37.10; Cu/Mn, 3.925. Found: C, 26.2; H, 1.05; N, 38.04; Cu/Mn, 3.999. For $C_{164}H_{128}Cl_{10}Mn_{19.8}O_{20}N_{192}Zn_{9.2}$ (**1-Zn^{2+}**·20CH_3OH) calcd: C, 27.54; H, 1.80; N, 37.60; Zn/Mn, 0.553. Found: C, 27.24; H, 1.35; N, 37.81; Zn/Mn, 0.546. For $C_{164}H_{128}Cl_{6.4}Li_{3.6}Mn_{25.4}N_{192}O_{20}$ (**1-Li$^+$**·20CH_3OH) calcd: C, 29.16; H, 1.91; N, 39.81; Li/Mn, 0.0168. Found: C, 28.62; H, 1.20; N, 39.83; Li/Mn, 0.0168.

Gas Adsorption Measurements. Adsorption isotherms were measured using a Micromeritics ASAP2020 instrument. Samples of **1-M** were transferred under a dinitrogen atmosphere to preweighed analysis tubes, which were then capped with a Transeal to prevent intrusion of oxygen and atmospheric moisture. The samples were evacuated by first heating to 150 °C at a rate of 0.2 °C/min and maintaining this temperature until the outgas rate was less than 2 mtorr/min. The evacuated analysis tubes were then transferred to an electronic balance and weighed to determine the mass of sample (typically 80−150 mg). The tubes were then transferred back to the instrument, and the outgas rate was again confirmed to be less than 2 mtorr/min. H_2 and N_2 isotherms at 77 K were measured using liquid nitrogen baths; H_2 isotherms at 87 K were measured using liquid argon baths. All

(9) (a) Kaye, S. S.; Long, J. R. *J. Am. Chem. Soc.* **2005**, *128*, 6506−6507. (b) Peterson, V. K.; Liu, Y.; Brown, C. M.; Kepert, C. J. *J. Am. Chem. Soc.* **2006**, *128*, 15578−15579. (c) Forster, P. M.; Eckert, J.; Heiken, B. D.; Parise, J. B.; Yoon, J. W.; Jhung, S. H.; Chang, J.-S.; Cheetham, A. K. *J. Am. Chem. Soc.* **2006**, *128*, 16846−16850.

Table 1. Composition and Gas Sorption Properties of Cation-Exchanged Compounds **1-M**

compd	formula[a,b]	M/Mn ratio (expt/found)	N_2 ads (cm^3/g)[c]	SA_{BET} (m^2/g)	SA_{Lang} (m^2/g)	H_2 ads (wt %)[d]	ΔH_{ads} (kJ/mol)[e]	color before/after desolvation
1-Mn^{2+}	$Mn_3[(Mn_4Cl)_3(BTT)_8]_2$[8]	N/A	547	2057(5)	2230(10)	2.23	5.5−10.1	colorless/colorless
1-Fe^{2+}	$Fe_3[(Mn_4Cl)_3(BTT)_8]_2 \cdot FeCl_2$	0.169/0.170	542	2033(5)	2201(10)	2.21	5.5−10.2	lt. green/brown
1-Co^{2+}	$Co_3[(Mn_4Cl)_3(BTT)_8]_2 \cdot 1.7CoCl_2$	0.210/0.210	563	2096(5)	2268(11)	2.12	5.6−10.5	pink/dk. blue
1-Ni^{2+}	$Ni_{2.75}Mn_{0.25}[(Mn_4Cl)_3(BTT)_8]_2$	0.121/0.121	554	2110(5)	2282(8)	2.29	5.2−9.1	lt. blue/brown
1-Cu^{2+}	$Cu_3[(Cu_{2.9}Mn_{1.1}Cl)_3(BTT)_8]_2 \cdot 2CuCl_2$	3.925/3.999	500	1695(5)	1778(10)	2.02	6.0−8.5	dk. green/black
1-Zn^{2+}	$Zn_3[(Zn_{0.7}Mn_{3.3}Cl)_3(BTT)_8]_2 \cdot 2ZnCl_2$	0.553/0.546	508	1927(5)	2079(9)	2.10	5.5−9.6	colorless/colorless
1-Li^{+}	$Li_{3.2}Mn_{1.4}[(Mn_4Cl)_3(BTT)_8]_2 \cdot 0.4LiCl$	0.017/0.017	530	1904(5)	2057(13)	2.06	5.4−8.9	colorless/colorless
1-Cu^{+}	$Mn_3[(Mn_4Cl)_3(BTT)_8]_2 \cdot 0.75CuPF_6$	N/A[10]	518	1911(5)	2072(11)	2.00	5.6−9.9	colorless/colorless

[a] Based on the relative ratio of M^{n+}/Mn^{2+} as determined using ICP-AA and on C, H, and N analysis. [b] For simplicity, guest solvents are omitted from these formulas. See the Experimental Section for the full molecular formulas. [c] Obtained at 77 K and 760 torr. [d] Obtained at 77 K and 900 torr. [e] Determined using a virial fit to the 77 and 87 K H_2 adsorption isotherms, as described in ref 8.

measurements and free space corrections were performed using UHP grade (99.999% purity) He, N_2, and H_2.

Inductively Coupled Plasma-Atomic Absorption (ICP-AA) Measurements. For the determination of M/Mn^{2+} ratios, samples of desolvated **1-M** were digested in concentrated nitric acid. Metals analyses were performed on a Perkin-Elmer Optima 3000 DV instrument.

Other Physical Measurements. Powder X-ray diffraction data was collected using Cu Kα radiation ($\lambda = 1.5406$ Å) on a Bruker D8 Advance diffractometer. Reflectance UV−vis spectra were collected on a Varian Cary 400 Bio UV−vis spectrophotometer with a Harrick attachment for solid samples. Thermogravimetric analysis (TGA) was carried out at a ramp rate of 1°/min in a nitrogen flow with a TA Instruments TGA 2950. Carbon, hydrogen, and nitrogen elemental microanalyses were obtained at the Microanalytical Laboratory of the University of California, Berkeley.

Results and Discussion

As an initial test for cation exchange, colorless crystals of solvated **1-Mn**$^{2+}$[8] were soaked in a saturated methanolic solution of anhydrous $CoCl_2$ and left undisturbed at room temperature. After 4 days, the crystals had turned pink and several rinses with fresh methanol did not diminish the intensity of the color, indicating the successful incorporation of Co^{2+} cations within **1**. Similar exchange experiments with $FeCl_2$ and $NiCl_2$ showed the incorporation of Fe^{2+} and Ni^{2+} ions, as revealed by gradual color changes to light green and light blue, respectively. In contrast, when colorless crystals of **1-Mn**$^{2+}$ were soaked in a saturated solution of $CuCl_2$, a much faster metathesis reaction was observed, and the crystals rapidly turned dark green. As expected, crystals of **1-Mn**$^{2+}$ remained colorless after soaking in saturated methanolic solutions of $ZnCl_2$, LiCl, or a solution of $[Cu(CH_3CN)_4](PF_6)$ in acetonitrile.

To determine the degree of cation exchange in **1-Mn**$^{2+}$, ICP-AA experiments were performed. Relative mass ratios of M/Mn determined using ICP-AA were then used in conjunction with C, H, and N analyses to calculate the chemical formula of each exchanged material. Unexpectedly, the Fe/Mn and Co/Mn ratios were found to exceed the stoichiometric ratio of 3:24 required for exclusive substitution of extraframework Mn^{2+} ions. The results indicate the inclusion of one extra equivalent of $FeCl_2$ in $Fe_3[(Mn_4Cl)_3(BTT)_8]_2 \cdot FeCl_2$ (**1-Fe**$^{2+}$) and 1.7 equiv of $CoCl_2$ in $Co_3[(Mn_4Cl)_3(BTT)_8]_2 \cdot 1.7CoCl_2$ (**1-Co**$^{2+}$). Conversely, in the case of Ni^{2+}, a slightly less than complete exchange of the guest cations led to the isolation of $Ni_{2.75}Mn_{0.25}[(Mn_4Cl)_3(BTT)_8]_2$ (**1-Ni**$^{2+}$). Notably, however, for the Cu^{2+} and Zn^{2+} samples, very large Cu/Mn and Zn/Mn ratios were observed. The large degree of exchange in these two cases may explain the fast and intense color change observed with Cu^{2+} and suggests that, along with the expected substitution of extraframework Mn^{2+} cations and possible adsorption of metal halides, a significant degree of intraframework cation substitution also occurs. Indeed, C, H, and N analyses support formulas of $Cu_3[(Cu_{2.9}Mn_{1.1}Cl)_3(BTT)_8]_2 \cdot 2CuCl_2$ and $Zn_3[(Zn_{0.7}Mn_{3.3}Cl)_3(BTT)_8]_2 \cdot 2ZnCl_2$ for **1-Cu**$^{2+}$ and **1-Zn**$^{2+}$, respectively.

Metathesis of **1-Mn**$^{2+}$ with salts of monovalent cations results in either very little exchange, as observed in $Li_{3.2}Mn_{1.4}[(Mn_4Cl)_3(BTT)_8]_2 \cdot 0.4LiCl$ (**1-Li**$^{+}$), or almost negligible substitution with Cu^{+}.[10] It should be noted, however, that in both cases complete substitution of extraframework Mn^{2+} requires incorporation of six monovalent cations per formula unit; confinement of these cations to the same space as that occupied by only three divalent cations may give rise to charge repulsion effects. Indeed, the total number of extraframework cations, including both charge-balancing and additional "adsorbed" species, is not larger than five, regardless of whether the exchange was effected with divalent or monovalent cations. In fact, the total number of extraframework cations is remarkably similar among all exchanged materials: 4.0, 4.7, 3.0, 5.0, 5.0, and 5.0 for **1-Fe**$^{2+}$, **1-Co**$^{2+}$, **1-Ni**$^{2+}$, **1-Cu**$^{2+}$, **1-Zn**$^{2+}$, and **1-Li**$^{+}$, respectively.

To remove the incorporated solvent molecules, fresh samples of **1-M** (M = Li^{+}, Cu^{+}, Fe^{2+}, Co^{2+}, Ni^{2+}, Cu^{2+}, Zn^{2+}) were heated under dynamic vacuum at 150 °C for approximately 48 h, a procedure that produced the best results with the parent material, **1-Mn**$^{2+}$.[8] Subsequent C, H, and N analyses of the desolvated materials confirmed that, as was the case with **1-Mn**$^{2+}$, approximately 20 solvent molecules remain bound to the framework following this treatment.[10] Color changes to brown, dark blue, brown, and black accompanied solvent evacuation in **1-Fe**$^{2+}$, **1-Co**$^{2+}$, **1-Ni**$^{2+}$, and **1-Cu**$^{2+}$, respectively, and indicated a change in the coordination environment of the adsorbed cations. Expectedly, **1-Zn**$^{2+}$, **1-Li**$^{+}$, and **1-Cu**$^{+}$ remained colorless upon solvent evacuation.

All exchanged materials retained the same crystalline structure as the parent framework, as revealed by powder X-ray diffraction patterns shown in Figure S9. As a further probe of the structural integrity of the frameworks, N_2 adsorption isotherms were measured for each of the exchanged, desolvated materials. The resulting N_2 uptake at 1 atm and 77 K ranged from 500

(10) ICP-AA indicated a very low Cu/Mn ratio of only 0.75:27. Although the solvent content of **1-Cu**$^{+}$ could not be determined reliably from C, H, and N analysis, a tentative formula of $Mn_3[(Mn_4Cl)_3(BTT)_8]_2 \cdot 0.75CuPF_6$ is provided to indicate the extent of Cu^{+} incorporation in **1-Mn**$^{2+}$. Incorporation of Cu^{+} into the parent compound was further tested by exposing a sample of desolvated **1-Cu**$^{+}$ to air. The initially colorless sample slowly turned light green-blue, as expected upon oxidation of Cu^{+} to Cu^{2+}.

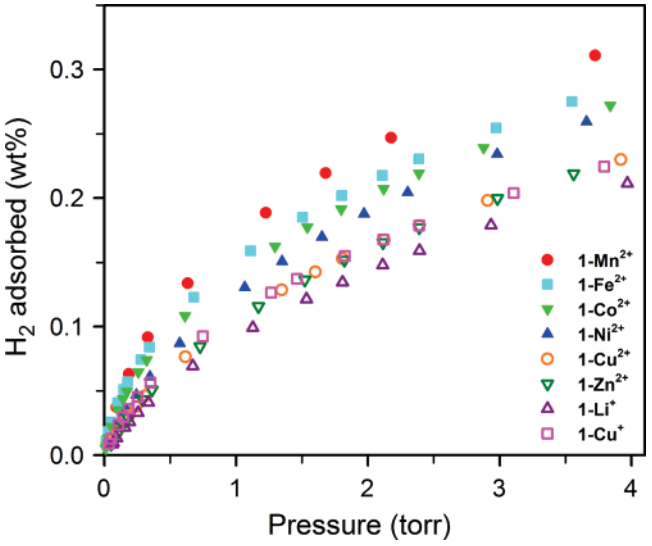

Figure 3. Low-pressure region of the H_2 adsorption isotherms for **1-M**, as measured at 77 K.

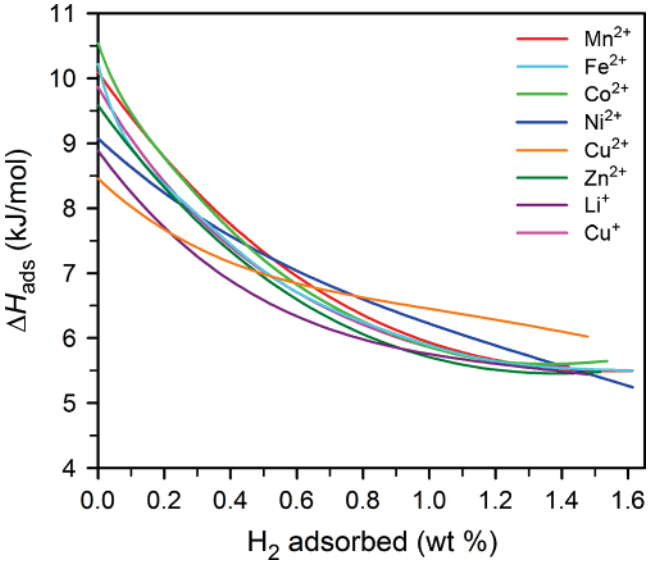

Figure 4. Coverage-dependent enthalpy of adsorption curves for the uptake of H_2 in compounds **1-M**.

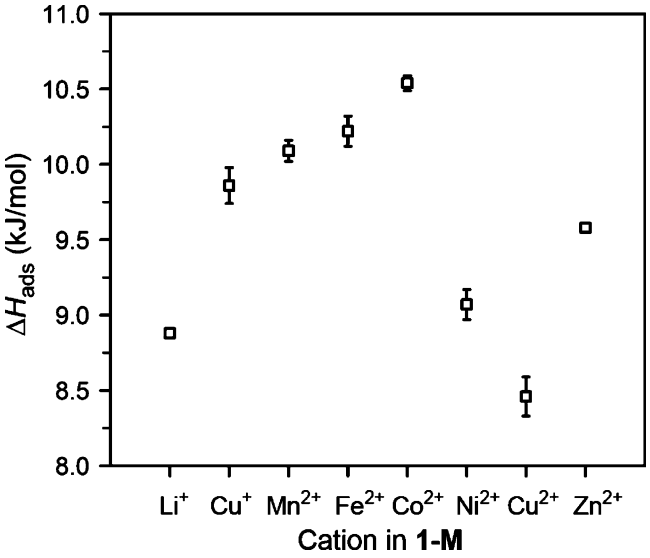

Figure 5. Zero-coverage values for the enthalpy of H_2 adsorption in compounds **1-M**. Error bars represent one standard deviation.

cm^3/g for **1-Cu**$^{2+}$ to 563 cm^3/g for **1-Co**$^{2+}$ (Table 1). Fitting the BET and Langmuir equations to each isotherm gave respective surface areas ranging from 1904(5) and 2057(13) m^2/g for **1-Li**$^+$ to 2210(5) and 2282(8) m^2/g for **1-Ni**$^{2+}$, while **1-Cu**$^{2+}$ showed significantly reduced values of 1695(5) and 1778(10) m^2/g, respectively. The comparatively low surface area of **1-Cu**$^{2+}$ may be attributed to partial collapse of the framework walls, which is likely due to incomplete reorganization of the $[M_4Cl]^{7+}$ clusters that ought to occur during the intraframework cation exchange. Indeed, even the small degree of intraframework cation exchange in **1-Zn**$^{2+}$ leads to BET and Langmuir surface areas of 1927(5) and 2079(9) m^2/g, somewhat lower than those of other materials exchanged with divalent cations. However, with the exception of **1-Cu**$^{2+}$, in which more extensive collapse presumably takes place, all materials exhibit surface areas very close to the BET and Langmuir values found for **1-Mn**$^{2+}$. This suggests that the framework and internal pore structure are retained upon cation exchange.

Further evidence of bulk framework integrity in the ion-exchanged materials arises from H_2 adsorption experiments. All materials show remarkably similar H_2 uptakes at 77 K and 900 torr, ranging from 2.00 wt % for **1-Cu**$^+$ to 2.29 wt % for **1-Ni**$^{2+}$ (Table 1). These results indicate that, as expected, a similar number of adsorption sites are available for a given material at a given set of temperature and pressure conditions. As shown in Figure 3, however, the H_2 isotherms show significant differences in the uptake slope at very low pressure. This suggests that at low coverage, for which H_2 molecules are expected to adsorb onto the strongest binding sites, the nature of the metal cation present within each material has a major contribution to the overall H_2-binding energy.

To assess the values of the H_2 adsorption enthalpies in these compounds, H_2 adsorption isotherms were also measured at 87 K. The 77 and 87 K data were then fit simultaneously using a virial equation previously utilized for analyzing materials with heterogeneous surfaces.[7k,8,11] As shown in Figure 4, the heat of adsorption curves display large variations at low H_2 uptakes and then increasingly similar values for H_2 coverages above 0.8 wt %, finally merging toward 5.5−6.0 kJ/mol at H_2 coverages of 1.5−1.6 wt %. It should be noted that, at 77 K, the available thermal energy is expected to promote H_2 adsorption at weaker sites even if stronger sites are not completely filled. It follows then that the measured value of ΔH_{ads} at a given H_2 coverage is in fact the average of the individual H_2-binding energies of all the occupied H_2 sites at that coverage. As such, in a given experiment, the H_2 adsorption enthalpy measured at infinitesimally low H_2 pressure will have the largest statistical contribution from the metal−H_2-binding site. Indeed, a comparison of these "zero-coverage" values, plotted in Figure 5, reveals a significant difference of 2 kJ/mol between the strongest and weakest H_2-binding materials in the series. The compound **1-Cu**$^{2+}$ shows an initial binding enthalpy of only 8.5 kJ/mol, while **1-Co**$^{2+}$ exhibits an enthalpy of 10.5 kJ/mol. The latter value is 0.4 kJ/mol higher than that of the parent material, **1-Mn**$^{2+}$, and is the highest H_2-binding enthalpy

(11) (a) Czerpiski, L.; Jagiello, J. *Chem. Eng. Sci.* **1989**, *44*, 797−801. (b) Jagiello, J.; Bandosz, T. J.; Putyera, K.; Schwarz, J. A. *J. Chem. Eng. Data* **1995**, *40*, 1288−1292. (c) Ansón, A.; Jagiello, J.; Parra, J. B.; Sanjuán, M. L.; Benito, A. M.; Maser, W. K.; Martínez, M. T. *J. Phys. Chem. B* **2004**, *108*, 15820−15826.

reported to date for a metal−organic framework. Although the different degrees of cation exchange prevent us from rigorously establishing an overall trend across the series, relative comparisons between subsets of exchanged materials provide important information about the nature of metal−H_2 interaction in each case.

Along these lines, the increasing binding energy trend observed for **1-Mn**$^{2+}$, **1-Fe**$^{2+}$, and **1-Co**$^{2+}$ may be attributable to the decrease in ionic radius in going from Mn^{2+} to Co^{2+} or possibly to the incorporation of additional metal cations within **1-Fe**$^{2+}$ and **1-Co**$^{2+}$. Note that no additional Ni^{2+} ions are adsorbed within **1-Ni**$^{2+}$, which shows a comparatively modest initial enthalpy of adsorption of 9.1 kJ/mol. On the other hand, the lower zero-coverage value for **1-Cu**$^{2+}$ of only 8.5 kJ/mol may be a consequence of the Jahn−Teller effect weakening the H_2 binding at Cu^{2+} sites within the framework, as previously observed in the isotypic phase $HCu[(Cu_4Cl)_3(BTT)_8]\cdot 3.5HCl$.[7q] Indeed, the trend in the heat of adsorption curve for **1-Cu**$^{2+}$, which surpasses those of other materials at higher H_2 coverage, is similar to that observed in this prior work and may likewise be associated with a more complete desolvation of the material. A different effect is observed in **1-Li**$^{+}$, wherein the monovalent cations can be expected to exercise a weaker electrostatic interaction with the H_2 molecules. Accordingly, **1-Li**$^{+}$ shows a relatively low initial binding energy of 8.9 kJ/mol, while **1-Cu**$^{+}$, which has minimal Cu^{+} incorporation, exhibits a zero-coverage value of 9.9 kJ/mol.

The larger binding energy observed for **1-Cu**$^{+}$ may also be attributed to the much stronger binding of H_2 previously observed for Cu^{+} in comparison to that of Li^{+}. For example, large bathochromic shifts of the H_2 stretching frequency indicated very strong adsorption of H_2 within Cu^{+}-exchanged ZSM-5,[12] in contrast with Li^{+}-exchanged ZSM-5, which adsorbed H_2 very weakly with a binding energy of 6.5 kJ/mol.[13] It is thus likely that doping of **1-Cu**$^{+}$ with an increased number of Cu^{+} ions may produce a material with an exceptionally large H_2 adsorption enthalpy.

The binding energy values obtained for **1-Li**$^{+}$ and **1-Cu**$^{+}$ also agree very well with theoretical studies of H_2 binding to Li^{+} or Cu^{+} ions. It has been estimated that bare Li^{+} ions should adsorb H_2 to form $[Li(H_2)_n]^{+}$ ($n = 1-6$) with estimated bond dissociation energies ranging from 23.9 to 9.3 kJ/mol in going from $[Li(H_2)]^{+}$ to $[Li(H_2)_6]^{+}$.[14] Moreover, calculations on Li^{+} ions complexed by other ligands, and thus somewhat closer to an experimental system, predict binding energies of 11.6 and 12.3 kJ/mol for the hypothetical species Li(CN)−H_2 and $[Li(CO)_3]^{+}$−H_2, respectively.[14] In agreement with the experimental observations, much larger binding energies of up to 56 kJ/mol have instead been calculated for H_2 adsorption onto Cu^{+}-exchanged chabazite,[12] further suggesting that Cu^{+}-rich metal−organic frameworks should exhibit very high H_2 adsorption energies.

To our knowledge, although there are numerous studies of H_2 complexation by Fe^{2+} and Ni^{2+}, especially in the context of [NiFe] and [Fe_2] hydrogenases, these studies provide no information regarding the binding energy between H_2 and Fe^{2+} or Ni^{2+} ions. Similarly, there are no estimations of the binding energy between Co^{2+} and H_2 molecules, although strong Co^{2+}−H_2 interactions have recently been characterized spectroscopically in Co^{2+}-exchanged ZSM-5.[15] Electronic structure calculations predict an enthalpy of 32.2 kJ/mol for the adsorption of H_2 onto Zn^{2+} sites within ZSM-5,[16] larger than that observed in **1-Zn**$^{2+}$. However, Zn^{2+}-exchanged ZSM-5 is known to promote heterolitic cleavage of H_2 rather than adsorption of molecular H_2,[16] such that an experimental value for the H_2 adsorption energy in this material has not been reported. In contrast, powder neutron diffraction experiments showed evidence of Cu^{2+}−H_2 interactions in $Cu_3[Co(CN)_6]_2$,[17] Cu_3(1,3,5-benzenetricarboxylate)$_2$,[9b] and $HCu[(Cu_4Cl)_3(BTT)_8]\cdot 3.5HCl$.[7q] The last of these compounds exhibited an initial binding energy of 9.5 kJ/mol, only slightly higher than that observed in **1-Cu**$^{2+}$ and not far from the 11 kJ/mol predicted for Cu^{2+}-exchanged mordenite.[18]

The foregoing results demonstrate that the anionic framework of a sodalite-type metal−organic solid can serve as a substrate for cation exchange, leading to variation of the H_2 adsorption enthalpy. Our findings, while somewhat complicated by the uneven degree of cation exchange across the series, show Mn^{2+}, Fe^{2+}, and Co^{2+} ions to yield the strongest H_2 binding among the cations assessed. Future efforts will focus on generating materials with an increased concentration of these metal ion sites and on exploiting the ion-exchange capabilities of **1-M** for applications in catalysis.

Acknowledgment. This research was funded by the General Motors Corporation. We thank the ITRI/Berkeley Research Center for providing a predoctoral fellowship to M.D. We thank Prof. A. Katz for use of the UV−vis spectrophotometer.

Supporting Information Available: A plot of the H_2 adsorption isotherms for **1-M**, reflectance UV−vis spectra, powder X-ray diffraction patterns, a TGA plot for **1-Mn**$^{2+}$, full tables of gas adsorption data, and tables of virial fit parameters. This material is available free of charge via the Internet at http://pubs.acs.org.

JA072871F

(12) Solans-Monfort, X.; Branchadell, V.; Sodupe, M.; Zicovich-Wilson, C. M.; Gribov, E.; Spoto, G.; Busco, C.; Ugliengo, P. *J. Phys. Chem. B* **2004**, *108*, 8278−8286.
(13) Otero Areán, C.; Manoilova, O. V.; Bonelli, B.; Rodríguez Delgado, M.; Turnes, P.; Garrone, E. *Chem. Phys. Lett.* **2003**, *370*, 631−635.
(14) Lochan, R. C.; Head-Gordon, M. *Phys. Chem. Chem. Phys.* **2006**, *8*, 1357−1370.
(15) Kazansky, V. B.; Serykh, A. I.; Bell, A. T. *Catal. Lett.* **2002**, *83*, 191−199.
(16) Shubin, A. A.; Zhidomirov, G. M.; Kazansky, V. B.; Van Santen, R. A. *Catal. Lett.* **2003**, *90*, 137−142.
(17) Hartman, M. R.; Peterson, V. K.; Liu, Y.; Kaye, S. S.; Long, J. R. *Chem. Mater.* **2006**, *18*, 3221−3224.
(18) Benco, L.; Bucko, T.; Hafner, J.; Toulhoat, H. *J. Phys. Chem. B* **2005**, *109*, 22491−22501.